Heritage Science

RESEARCH

Open Access

Identification of an unusual pale green material on the surface of an ancient Chinese bronze vessel and application of laser cleaning to its removal

Yijia Shen[1*], Guangmin Zhang[1] and Xinguang Zhou[1]

Abstract

An ancient Chinese bronze vessel represented a typical difficult situation for conservation: a large quantity of an unwanted pale green material of unknown nature adhered to a surface fully decorated with delicate relief. The diagnostic itinerary, beginning with in-situ Raman spectroscopy analysis and followed by scanning electron microscopy-energy dispersive spectroscopy and X-ray diffraction, was found to be advantageous in revealing the presence of both inorganic and organic compounds in the pale green material. Irradiation with pulsed Nd:YAG 1064 nm laser in LQS regime (100 ns) followed by chemical cleaning using a low-toxicity solvent mixture proved to be respectful towards the original patina of the bronze as well as of high efficiency. Tentative analyses with the Raman spectroscopy and hyperspectral imaging were conducted to provide further indications on quality and visual effect during the cleaning result assessment. In parallel with the analyses and interventions on the bronze vessel, experiments were also carried out on mock-up samples in order to further explore the Raman scatter property and reactivity with laser ablation of mixed materials. The study provided reference for the optimization of diagnostic and conservation for the bronze artwork with similar situation.

Keywords Bronze artwork, Raman spectroscopy, Laser cleaning, Hyperspectral imaging, Art conservation

Introduction

For bronze artwork cleaning, challenges frequently encountered include: the unwanted materials sometimes having complicated nature difficult to identify, the wide presence of surface cavities and fissures hard to clean inside but easy to retain external materials, and the substrate to conserve with historicized patina often mechanically and chemically sensitive [1].

Tackling all these concerns, the present work is an exploration of both analytical itinerary and intervention strategy. A precious ritual bronze *Gu* (wine vessel) of late Shang Dynasty (1600B.C.–1046B.C.) of Shanghai Museum was examined here, on which an unusual pale green material was widely found inside the submillimetric-sized cavities of the relief over the whole surface. Instead of beginning with X-ray diffraction (XRD) analysis most commonly used for corrosion products recognition, the identification of this material took the non-destructive in-situ Raman spectroscopic investigation as the first analytical step, which is capable of revealing both inorganic and eventual organic compounds without sampling. Interpretation of the unusual Raman spectra obtained were assisted with the following analyses with scanning electron microscopy-energy dispersive spectroscopy (SEM–EDS), and further verified with XRD analyses.

*Correspondence:
Yijia Shen
shenyijia@shanghai-museum.org
[1] Conservation Center, Shanghai Museum, 1118 Longwu Road, Shanghai 200231, China

Conventional cleaning methods proved to be inadequate in this case. The application of Nd:YAG 1064 nm laser, as the most commonly used laser type in conservation laboratories and for metal cleaning [2, 3], was then investigated according to the identified composition of the target material. For the inefficiency of removing typical corrosion products and induction of surface discoloration, as often reported in the experimental studies on coins, small archaeological fragments or mock-up samples [4–7], laser cleaning is still not universally accepted for bronze cleaning [8]. However, the existing reports on real conservation task, mostly of outdoor bronze monuments but also museum collections are few in number but demonstrated significant potential of this method [9–13], used alone or in combination with other methods, in safe and efficient removal of thin corrosion products, environmental contaminants, aged restoration materials and derived degradation products, while convenience in cleaning surface with very complicated morphology is also observed [12, 14]. In the present study, adoption of laser was based on programmed comparative tests, while efforts were made towards both optimizing the laser operation on tridimensional object of extensive surface, and finding the ways to study the mechanism of laser-material interaction, with the aim of providing practical reference in a broader sense.

Moreover, multiple evaluation methods were explored to assess the cleaning results not only in qualitative dimension but also on general visual effect, of which the latter is often neglected in the laboratory studies. Besides routine microscopic observation, tentative analysis of Raman spectroscopy was adopted to evaluate the results on micro area on chemical level. The hyperspectral imaging increasingly used in artwork conservation field for the assessment of condition as well as the recognition of material and concealed information was also experimented here [15, 16]. As a method capable of acquiring material information in a wide spectral range and provide intuitive material distribution mapping based on their spectral data [17–19], it was used to assess the surface condition and visual effect of larger area, for which the direct observation and daylight photography have been so far the only commonly adopted methods.

Despite the case-specificity of artwork, this work was aimed at providing indications on the optimization of diagnosis and cleaning for bronze artwork surface with similar complicated situation.

Background

This *Gu* vessel of square section is of considerable dimension (height circa 36 cm) and shows significant morphological complexity with typical delicate relief decoration covering almost all the surface (Fig. 1a).

Whether any intervention had been done to it before it was acquired by the museum was unknown. The alloy is leaded tin copper according to the analysis previous to this work through portable X-ray fluorescence, which revealed the contents of copper ranging from 59 to 77%, tin from 8 to 13% and lead from 12 to 16%. Although showing lead content higher than the most classic recipe for ritual bronze, this alloy composition is still in line with some reported archaeological findings of the same era [20, 21].

The bronze appeared to be in good condition with a homogenous metallic brown surface showing notable gloss. Typical stable patina including cuprite, malachite and azurite were widely present with varying thickness, from very thin layer to accumulation of almost half millimeter in height, which also appeared glossy. No obvious earthen contaminants were observed, however, legibility of the object was heavily obscured by the extensive presence of the before-mentioned material of unknown nature, which seemed to have a powdery-like consistency. Its pale green color raised concern of the detrimental "bronze disease", the corrosion products of chlorides [22] (Fig. 1b). This material was immediately identified as the target of removal.

Materials and methods

Microscopic observation

Microscopic observation was conducted in the preliminary investigation and later in evaluating the cleaning effects of different methods. Both a desktop Keyence VHX-5000 and a portable Dino-lite AM73915MZT were used on account of the complicated shape of the object.

Qualitative analysis

Raman spectra of typical areas with deposit before and after laser cleaning were acquired with a Renishaw inVia™ InSpect confocal Raman microscope, using an Nd:YAG 532 nm excitation through fiber-optic probe connected to an objective of 50x. Nominal laser power of 532 nm (25 mW) was reduced to 10%, 5% and 1% according to the yield of specific tested area. Data were first acquired by static scan in the range from 60 to 1840 cm^{-1}, which was usually used for inorganic compounds, with exposition time from 5 to 20 s and repeated acquisitions from 10 to 40 times to better the signal to noise ratio. After obtaining more spectra demonstrating probable presence of organic compounds, extended scan in the range from 100 to 3200 cm^{-1} was performed for some areas with the exposition time of 20 s.

The SEM analysis was conducted with a FEI Quanta650 FEG scanning electron microscope. The analysis was carried out with secondary electron detectors, high vacuum mode, and accelerating voltage

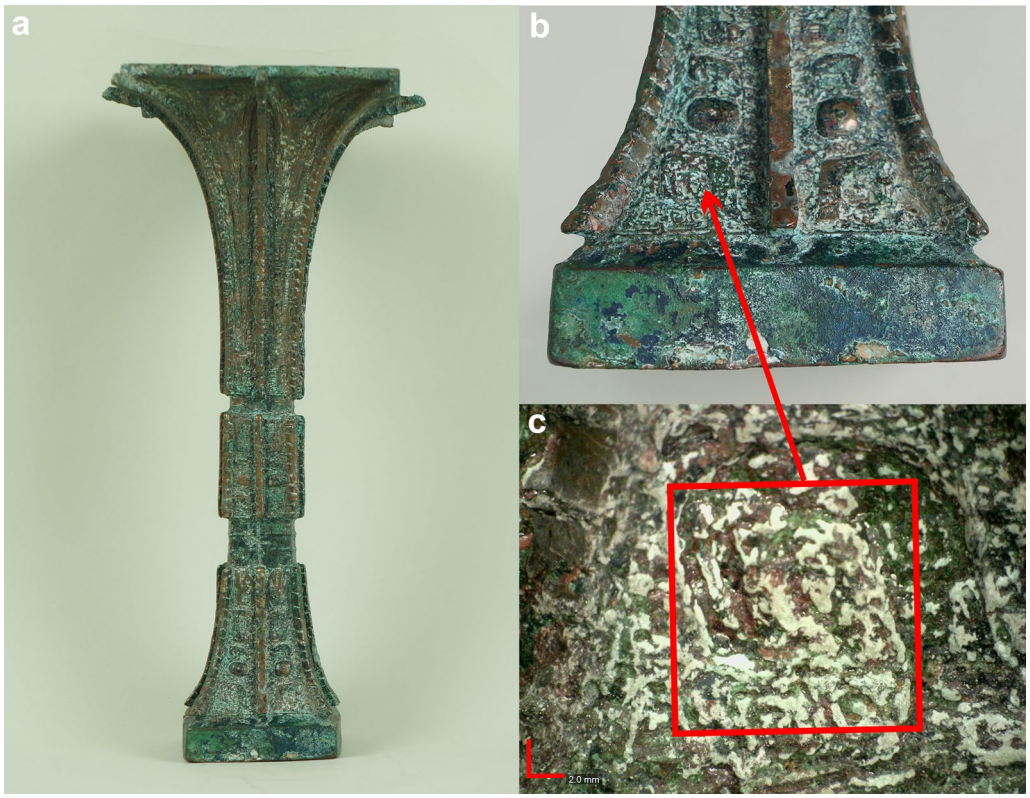

Fig. 1 **a** The square bronze *Gu* vessel with a total height of circa 36 cm. **b** Lower part of the *Gu* vessel. **c** Enlarged view of an area shown in (**b**) demonstrating concentration of pale green material in micro cavities. Area of the red square: circa 1 cm^2. Scale bar in (**c**): 2.0 mm

15 kV. The EDS data were acquired with an Oxford INCA energy-dispersive X-ray spectroscope, using excitation voltage 20 kV with spot mode.

The instrument employed for XRD analysis was a Rigaku D/MAX 2550 X-ray diffractometer, using Cu Kα radiation, 40 kV/100 mA, angle range from 5 to 90°, and at a step length of 0. 02°.

Conventional cleaning agents

Hand tools of scalpel, needle and brush, and a 25 kHz ultrasonic scaler, Desply Cavitron® BOBCAT® were used for mechanical cleaning trial.

According to the results of the qualitative analysis, the chemical agents targeting to the identified inorganic phase were disodium, trisodium and tetrasodium salts of ethylenediaminetetraacetic acid (EDTA) at the concentration of 5% in water (w/v), with pH values equal to 4.7, 7.1 and 11.2 respectively. For the dissolution of organic phase, two ternary solvent mixtures were formulated through online tool *INTERACTIVE SOLVENT AND SOLUBILITY TRIANGLE*© developed by the Istituto Centrale per il Restauro of Italy [23].

Laser cleaning setup

The adopted El.en EOS Combo 1064 nm Nd:YAG laser cleaning machine has a flexible deliver system using optical fiber and allows working in both short free running (SFR) regime (pulse width from 30 to 110 μs) and long Q-switched (LQS) regime (pulse width of 100 ns). The attenuator lenses of lower transmittance reducing the nominal energy to 25% and 50% were used. These accessories of the same supplier are designed to be interchangeable with the lens cover on the end of the handpiece through simple screwing.

Hyperspectral imaging

A Themis Vision Systems NUV-NIR 350 portable scanning hyperspectral imaging camera was used to capture the hyperspectral data at different wavelength bands from 350 to 1000 nm at a spectral resolution of 1.5 nm. The imaging spectrometer is equipped with the PCO edge 5.5 sCMOS camera, illuminated by two halogen lamps, and the field angle is 30 degrees. The standard white board data and dark current data were obtained simultaneously during each scanning for the radiometric

calibration. This instrument was applied to selected test area before and after cleaning.

Mock-up sample

In order to verify the interpretation of obtained Raman spectra and the mechanism of laser-material interaction, mock-up samples comprising powdery form of the substances found in the pale green material were made through the Shimadzu MP-35 briquetting machine. The powders were premixed thoroughly and then pressed inside a plastic sample holder under the pressure of 30 tons for 30 s. The prepared sample was a compact round disk with about 3.5 cm in diameter and 3 mm in thickness.

Results

Preliminary analysis

The pale green substance showed granular textures under microscope, different from the fine and homogeneous texture of chlorides corrosion [24] (Fig. 2). In more, this substance did not collapse at the touch of manual tools as normal powdery corrosions; instead, it was compact and firmly embedded inside the cavities.

The exterior surface uncovered from this substance presented stable patina with an unusual luster and felt very smooth, contrasting drastically with the coarse and dull aspect of the inner part of the vessel. The microscope imaging under raking light revealed parallel linear traces from the exposed lustrous zones, indicating mechanical working traces of polishing and flattening (Fig. 3), most probably left by agate spatula frequently used in the past on Chinese bronze to enhance the surface luster [25].

The Raman spectra obtained from different areas of the pale green product were relatively similar (Fig. 4), but did not match those of any known bronze corrosion products. The bands commonly found below 1000 cm^{-1} were centered at ~ 379 cm^{-1}, ~ 418 cm^{-1} and ~ 474 cm^{-1}, among which the last one was usually the most intense. Weak signals centered at ~ 148 cm^{-1}, ~ 219 cm^{-1}, ~ 575 cm^{-1}, ~ 645 cm^{-1} and ~ 750 cm^{-1} were sometimes observed. The bands over 1000 cm^{-1} are often attributed to the functional groups of organic materials: skeletal C–C stretching (~ 1060 cm^{-1}

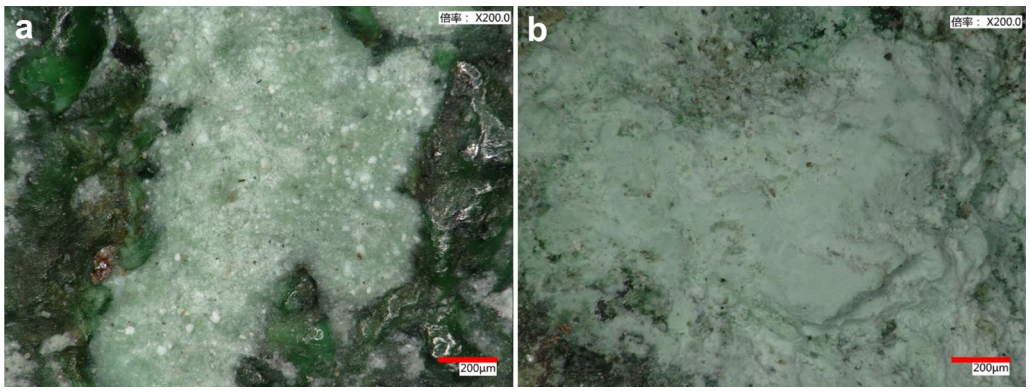

Fig. 2 **a** Granular texture of the pale green material on the *Gu* vessel. **b** Chlorides corrosion on another bronze. Scale bar: 200 μm

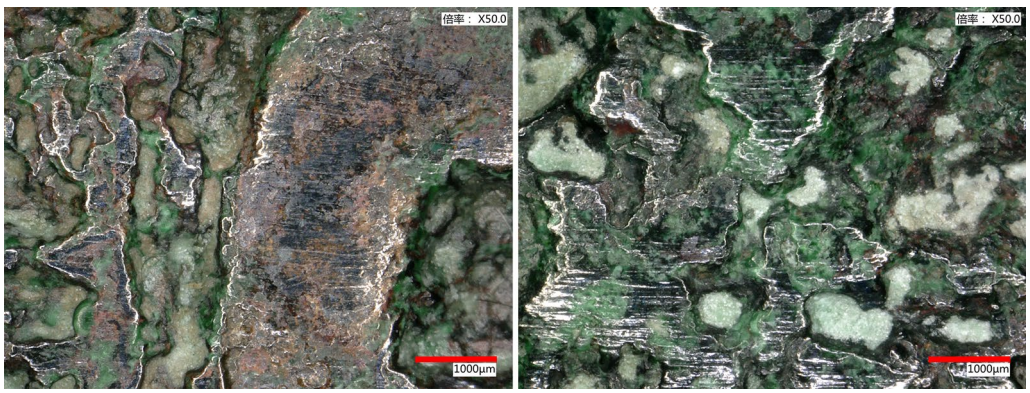

Fig. 3 Surface patina polished and flattened, showing parallel linear traces. Scale bar: 1000 μm

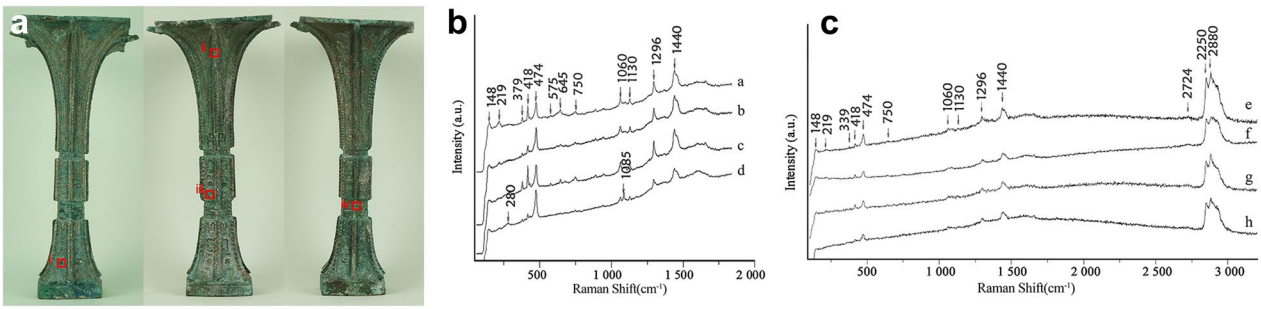

Fig. 4 Raman spectra of the pale green material obtained from various areas. **a** Testing areas on different faces of the objects from which the spectra of static scan in (**b**) and of extended scan in (**c**) were obtained. Area i: spectra a and e; area ii: spectra b and f; area iii: spectra c and g; area iv: spectra d and h

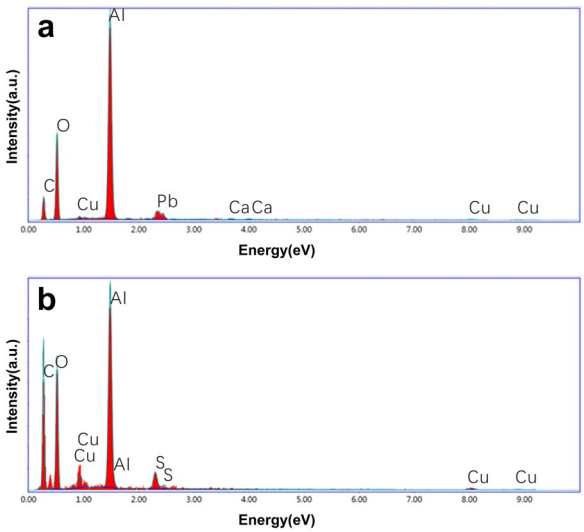

Fig. 5 EDS results of two test areas demonstrating the presence of lead, sulfur and calcium

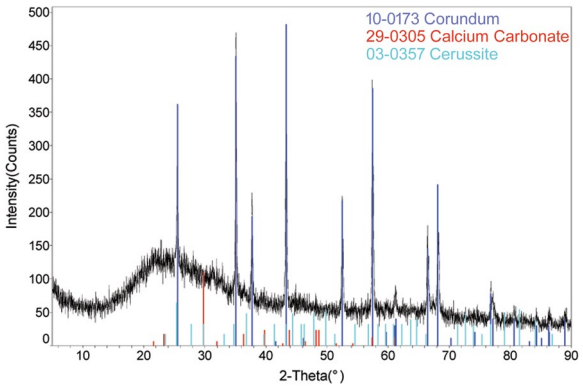

Fig. 6 XRD pattern of the sample

and ~ 1130 cm^{-1}), CH_2 twisting (~ 1296 cm^{-1}), CH_2 and CH_3 bending (~ 1440 cm^{-1}), and C-H stretching vibration mode (~ 2724 cm^{-1}, ~ 2850 cm^{-1} and ~ 2880 cm^{-1}) [26, 27, 28]. However, scrubbing repetitively the object surface with ethanol-soaked or acetone-soaked cotton swabs, no sign of the presence of organic product (dissolution, swelling or just turning sticky) was revealed.

The following SEM–EDS analysis revealed a surprising quantity of aluminum in the green material: around 30% (wt.) in average and sometimes over 50%, much higher than it could be in usual earthen contaminants. The content of oxygen was alike, or even higher than aluminum. Carbon (circa 20% in average) and copper were also present, and the content of the latter was usually around 5% but could be up to over 30% in some spots. Other elements frequently found were sulfur, lead, calcium and sometimes also silicon, which usually had the concentration below 2% except for lead. The concentration of lead varied notably from 1% to over 10% (Fig. 5).

This unusually high content of aluminum is most likely due to contamination. A common conservation material containing aluminum is the abrasive corundum powder, which can be applied through sand blasting or manually with cotton swab or cloth. Considering that abrasion with corundum powder would result in a "matte" aspect, the agate spatula might be a follow-up intervention to recover the surface luster.

The presence of corundum was confirmed by XRD analysis. Moreover, calcium carbonate and cerussite were also revealed sometimes (Fig. 6). All the obtained spectra demonstrated noisy background. This indication of poor crystallinity could also result from eventual presence of organic materials.

This cross information allowed the interpretation of the Raman spectra. The peaks centered at ~ 379 cm^{-1}, ~ 418 cm^{-1}, ~ 575 cm^{-1}, ~ 645 cm^{-1} and ~ 750 cm^{-1} are consistent with the spectra of corundum [29, 30], among which the ~ 418 cm^{-1} corresponds with the A_{1g} vibration modes and the others correspond to the internal

and external E_g vibration [31, 32]. Weak shifts sometimes found at ~ 280 cm^{-1} and ~ 1085 cm^{-1}, as shown in Fig. 4d, are attributable to calcite ($CaCO_3$), while the bands of low wavenumber at ~ 148 cm^{-1} and ~ 219 cm^{-1} might be due to the penetration of laser to the cuprite (Cu_2O) of the substrate, which are attributable to the E_u mode and $2E_u$ mode respectively [33, 34]. It is difficult to determine if cerussite ($PbCO_3$) were also revealed with Raman, since its characteristic peak centered at ~ 1054 cm^{-1}, attributable to the CO_3^{2-} v_1 stretching vibrations [35, 36] is close to that centered at ~ 1060 cm^{-1} frequently found here.

The confusing strong peak centered at ~ 474 cm^{-1} revealed in almost all the spectra obtained and, in most cases, more intense than the characteristic band centered at ~ 418 cm^{-1} of corundum, was probably attributable to the S–S stretching vibration mode of covellite (CuS) [37, 38], considering that sulfur was also revealed with SEM–EDS. The corundum powder for abrasion, α-Al_2O_3, is reported to have relatively weak characteristic first-order Raman spectrum [30].

Spectra obtained from the mock-up samples (see Fig. 11) demonstrated that for covellite, even at the concentration as low as 1% (wt.) in the mixture with corundum or with corundum and cerussite, the characteristic peak at 474 cm^{-1} was still found to be very strong (Fig. 7). This concentration was already lower than what was revealed with SEM–EDS. The reason why XRD failed to reveal its existence might be the sampling bias, the low concentration or signal overlap. Actually, the greenish tones of the examined substance must be due to some forms of copper ion that immigrated from the substrate, and covellite might not be the only one.

It was then reasonable to take the bands in the range over 1000 cm^{-1} as a separate spectrum, which was found to be very similar with the spectra of some polymers in the Renishaw database of instrument: poly (ethylene-*co*-acrylic acid), poly (ethylene-*co*-ethyl acrylate), poly (ethylene-*co*-vinyl acetate) and poly (ethylene-*co*-methyl acrylate-*co*-acrylic acid). These materials are all easily found in market and can be the main component of some surface protectives. This also explained why the seemingly powdery substance was remarkably compact and adherent.

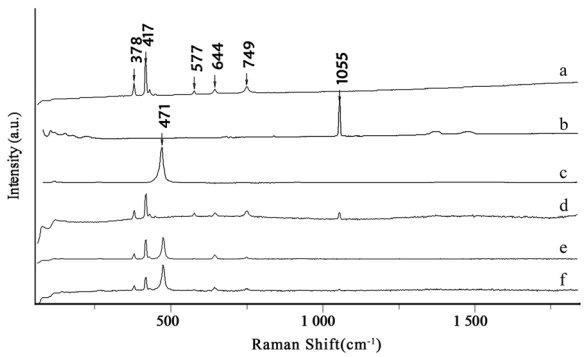

Fig. 7 Raman spectra of mock-up samples: **a** pure corundum, **b** pure cerussite, **c** pure covellite, **d** 1% (wt.) cerussite in corundum, **e** 1% (wt.) covellite in corundum, **f** 1% (wt.) cerussite and 1% (wt.) covellite in corundum

In the end of the preliminary analysis, it could be concluded that the examined material is a multi-phase mixture mainly composed of corundum powder and polymer. They are results of two different interventions, one for corrosion removal or surface polishing and the other for surface protection. It is impossible to know whether the corundum powder adhered to the residue of protective or the polymer was applied intentionally to the cavities where the residual corundum powder was mistaken as active corrosion products. The minor composition includes calcite (environmental contamination), cerussite (corrosion products of bronze) and probably covellite and other forms of copper ion or copper compounds. It was decided against further efforts on the identification of exact polymer type or the verification of the presence of covellite and eventual other minor composition, since the data obtained so far were sufficient for the consequent reasoning of intervention strategy: the deposit substance had to be removed in a way of high spatial precision, "broad-spectrum" to act on different phases and free from the concern of leaving further residue. The lustrous patina, in spite of being result of intervention, was already historicized and must be kept unaltered during the intervention.

Cleaning tests

Mechanical cleaning

The typical width of the gaps of the relief decoration filled with the multi-phase deposit were about 0.4 mm, while many cavities were even smaller. Cleaning with manual tools meant “digging out” this compact substance from numerous cavities, which was extremely time-consuming and prone to leave scratches. As for the ultrasonic scaler with which one could work faster, the flat-head insert cleaned efficiently the surface with less irregularity, such as the flat surface of the edge of the vessel’s mouth, but proved to be ineffective for the cavities of small dimension in relief decoration. The pin insert was found to be dangerous for tending to drill into the depth and damaging the patina (Fig. 8).

Chemical cleaning

Mixtures comprising of both organic and inorganic compounds, as revealed with Raman spectroscopy in this case, are particularly difficult to remove chemically, since most of the chemical agents used for bronze conservation

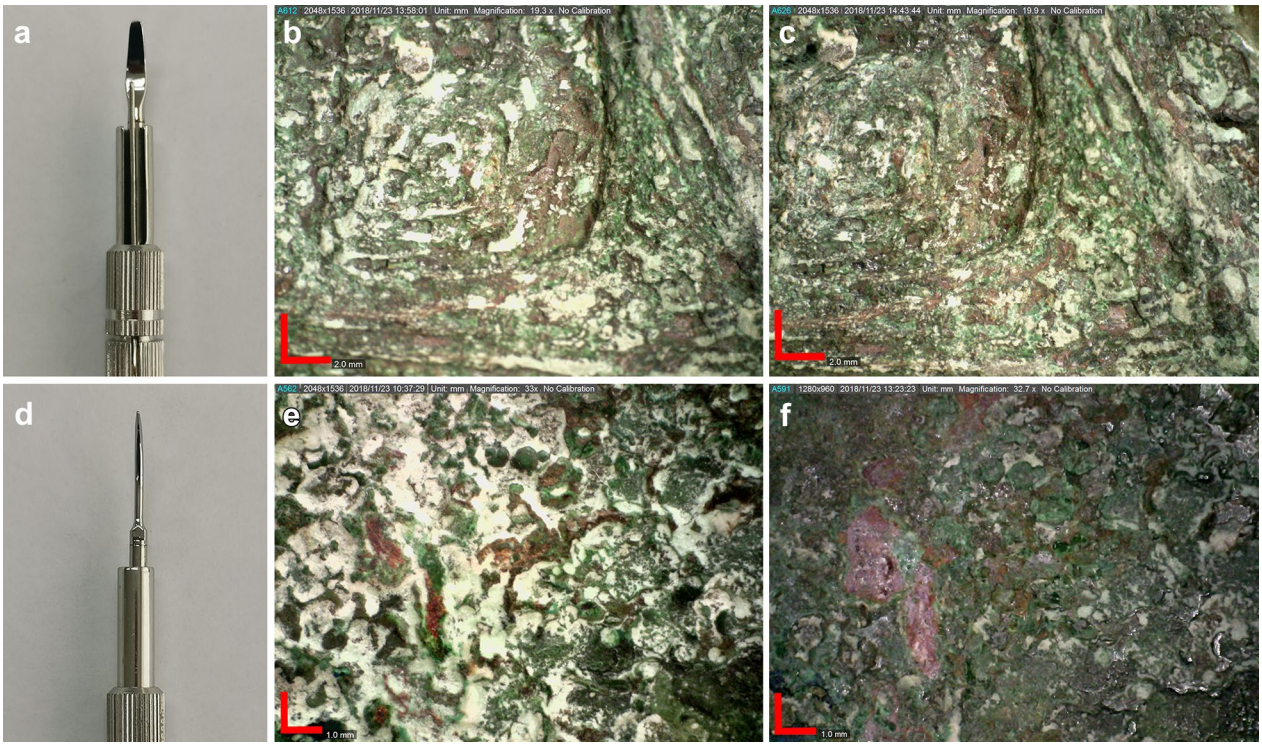

Fig. 8 **a** Insert with flat-head. Area before (**b**) and after cleaning with flat-head insert (**c**), scale bar: 2.0 mm. **d** Pin insert. Area before (**e**) and after cleaning with pin insert showing excessive cleaning (**f**), scale bar:1.0 mm

work on either inorganic or organic phase. Acids and chelants are traditionally used for removing inorganic phases [39, 40], while organic solvents are commonly applied to dissolving organic matters [41–43]. Few single chemical agents capable of working on both phases, such as strong inorganic acids, are unacceptable to the conservation. The strategy in this work was to dissolve or extract one of the phases to provoke the structural collapse of the whole mixture, as observed on industrial metal–organic frameworks in the presence of water or organic solvents [44–46].

The first option was to remove the aluminum oxide chemically stable and insoluble in water. A commonly used method is using the chelating agents to form chemically stable connection with transitional metal ions [47], as reported in many studies on corrosion removal [48–52]. Among them, the chosen EDTA sodium salts aqueous solutions are widely used in bronze surface cleaning through chelation with various metal ions, such as

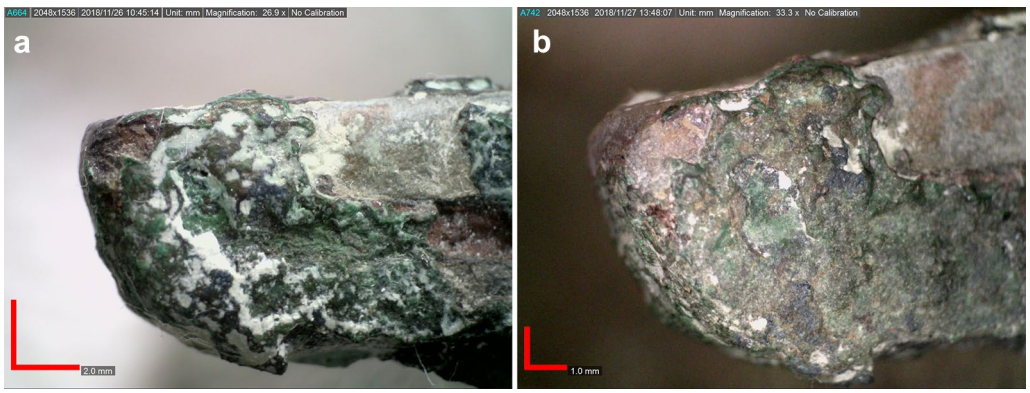

Fig. 9 Before (**a**) and after (**b**) cleaning with 5% EDTA-3Na in deionized water. Scale bar: 2.0 mm (**a**) and 1.0 mm (**b**)

those of copper, calcium and aluminum [50–56]. All the bisodium, trisodium and tetrasodium EDTA solutions worked already at the concentration of 5% with wet compress for 10–15 min. However, the chelation happened even faster on the surrounding bronze surface than on the green material and led to an evident discoloration of the patina (Fig. 9). The process was hence considered not selective and actually uncontrollable. Obviously, any other commonly used liquid agent would create the same risk for the inevitable diffusion to the surrounding areas even with supporting materials, considering the submillimetric dimension of these cavities. Moreover, residue of the aqueous agents must be removed thoroughly with laborious and invasive operation, such as repetitive wet compress with water, which could introduce further risk to the object. These efficient but risky agents were therefore excluded.

The alternative was to dissolve the polymer phase with organic solvents nonreactive for the bronze substrate. In order to lower environmental and health hazards, ternary solvent mixtures of low toxicity were formulated through the open-source software *INTERACTIVE SOLVENT AND SOLUBILITY TRIANGLE*© developed specifically for the conservation field, an interactive tool based on the Teas solubility graph with automatic calculation module. Its database includes both the solubility parameters of toxic organic solvents to be substituted and the "solubility area" (a congregation of solubility parameters) of conservation materials to remove or dissolve (e.g., consolidant, protective, adhesive, etc.) (Fig. 10a). Two formulas were prepared with low-volatile solvents of isopropyl alcohol, nonane and methyl ethyl ketone in different proportions. The first mixture composed of 43% isopropyl, 18% nonane and 39% methyl ethyl ketone had the same solubility of tetrahydrofuran, a very strong but toxic solvent. The solubility parameters of the second, which was composed of 14% isopropyl, 47% nonane and 39% methyl ethyl ketone, was located in the center of the solubility area of a poly (ethylene-*co*-vinyl acetate) material, Elvax 40W. This product was the closest in nature to the organic phase of the examined material among all the materials in the database.

The low volatility of these formulas permitted the application of wet compresses, while drops of solvents were added into compresses every 5 min. Both formulas began to work after about 30 min, leaving the green material increasingly loose, but showing no further improvement over one hour. It was difficult to verify whether the polymer was dissolved or just swelled. Unlike the easy removal when using the EDTA sodium solutions, laborious brushing was needed after the treatment of organic solvents, during which a large quantity of the deposit substance diffused to the surrounding areas (Fig. 10b), leaving the surface a whitish aspect even after following repetitive cleaning. This method was considered only suitable for a small quantity of material to remove.

Laser cleaning

Different from the laser cleaning for bidimensional object as painting, for which electromechanical platform could be used [57], the cleaning of tridimensional object with uneven surface has to be conducted through manually operating the handpiece as using other hand tools. This is a flexible process with less precision in irradiation

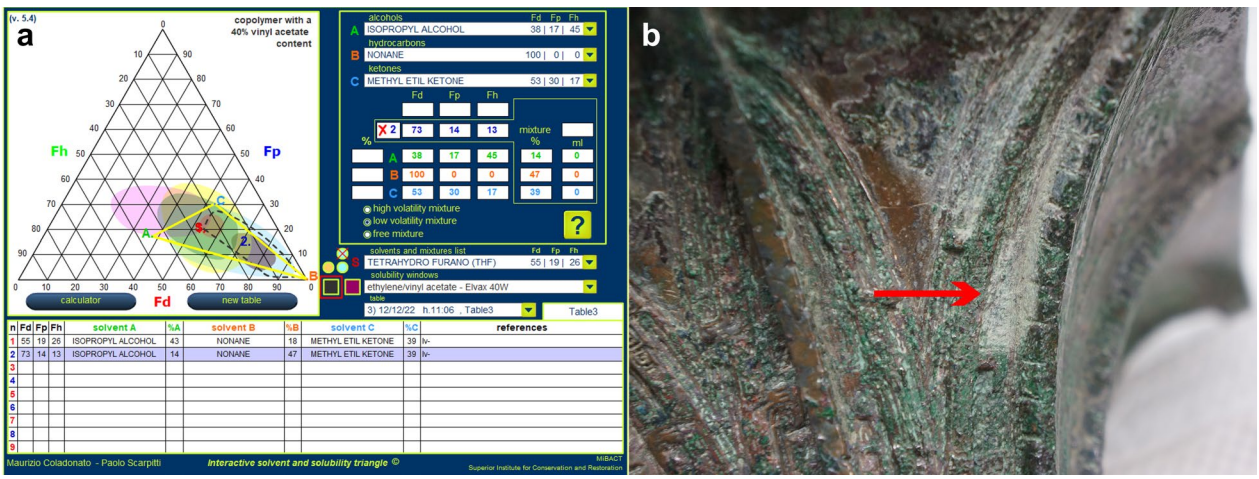

Fig. 10 **a** Interface of the software. The red point "1" representing the first formula overlaps the point "S" representing the tetrahydrofuran. The blue point "2" representing the second formula is located in the center of the solubility area of Elvax 40W, defined by the black dotted line. In the table are reported volumetric proportions of solvents used for the two formulas. **b** The pale green material spread to the surrounding area during the cleaning with organic solvents

fluence. To limit the laser beam irradiation to the target material and reduce risk of damage, the set smallest beam spot of 1 mm in diameter was chosen but used slightly out of focus up to around 1.5 mm in diameter. According to the literature and the experience of the operator, smaller spot leads to more intense interaction than bigger one at equivalent or even lower fluence, the out-of-focus mode could avoid excessive removal and sharp spot sign, making the cleaning effect more homogeneous [58]. Considering that the underneath situation and the thickness of the unwanted material were unknown and could vary from point to point, this operation also left space for the manual adjustment of working distance and fluence.

Initial tests were limited to the less obtrusive areas trying both of the two pulse widths, following a sequence from the lowest to higher fluences, and with both wet and dry cleaning. Attenuators were used to reduce the laser fluence. It was found that at the lowest energy of 37.5 mJ (obtained through selecting the set minimum energy scale of 150 mJ and using 25% attenuator) with LQS regime, from 2 to 6 pulses could remove most of the deposit materials of a single irradiated area in most cases. At the above-mentioned spot diameter, the fluence was 2.1 J/cm^2, while the manual operation induced variation in spot size and consequent fluctuation in fluence around ± 30%. Wetting the surface with the mixture of water and ethanol (1:1 v/v) could improve the ablation and reduce discoloration risk of the exposed substrate. The frequency adopted was 2 Hz, with which efficient ablation was obtained and necessary movement of beam was possible, while further heating derived from high frequency could be avoided [59]. After obtaining satisfactory results on micro zone, the trial was extended to larger area. The surface after cleaning appeared much more readable without alteration of color or gloss (Fig. 11).

It was verified that even for the cavities smaller than the beam diameter, with the out-of-focus mode, the Gaussian pulse left the patina of surrounding bronze surface intact, of which the irradiation declined from the center to the margin. Using the same working parameter on different types of glossy patina typically found on this bronze, it was observed that within 2 pulses, the substrate was actually unaltered. Five pulses could induce very slight discoloration almost negligible, while 10 pulses could remove some malachite patina (Fig. 12). Therefore, at this fluence with controlled pulse number and timely movement of handpiece, the laser irradiation was in general safe to this bronze. Although it was impossible to define the exact destructive threshold of substrate due to the significant inhomogeneity of the surface, these experiments gave important indications for practice that when most of the

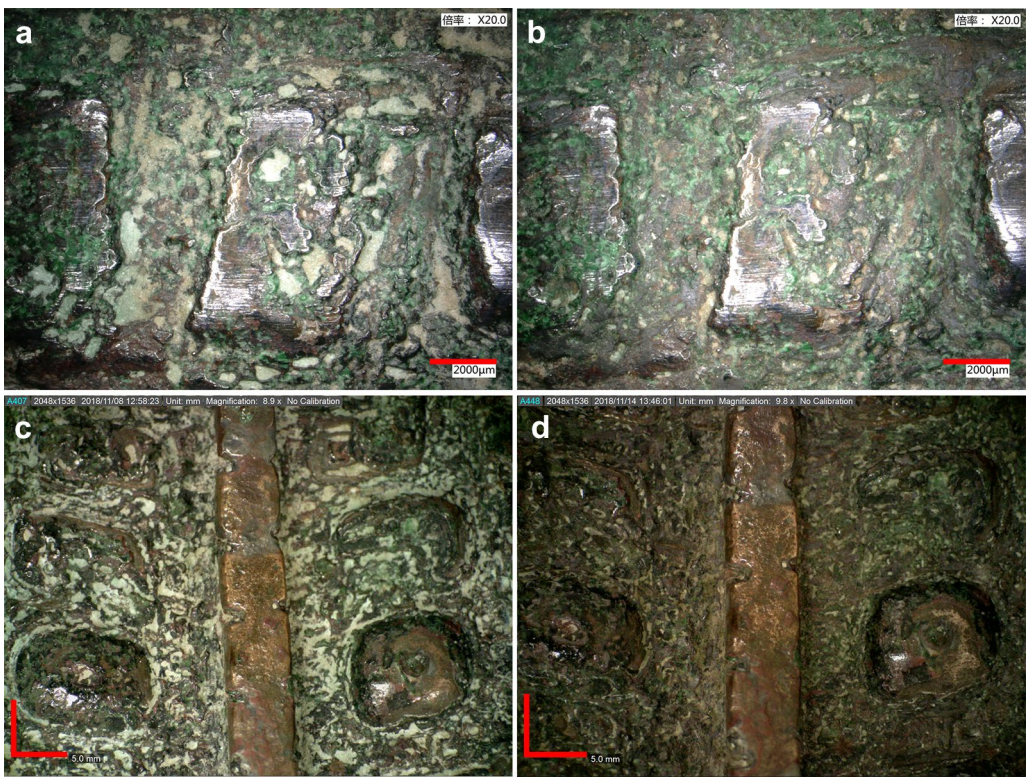

Fig. 11 Before (**a**, **c**) and after (**b**, **d**) laser cleaning of test areas. Scale bar: 2000 μm in (**a**) and (**b**), 5.0 mm in (**c**) and (**d**)

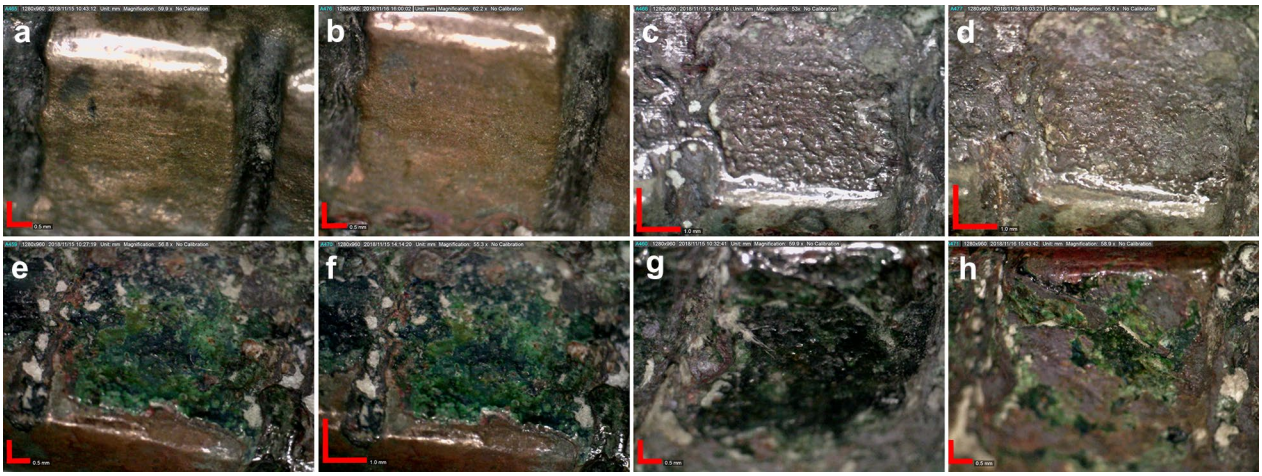

Fig. 12 Before (**a**, **c**, **e**, **g**) and after (**b**, **d**, **f**, **h**) laser cleaning of test areas, which received 2, 5, 5 and 10 pulses respectively. Scale bar: 0.5 mm in (**a**, **b**, **e**, **g**, **h**), 1.0 mm in (**c**, **d**, **f**)

pale green material was removed and the substrate began to expose, the operation should stop within 2–3 pulses.

Localized micromelting considered as the cause of the surface discoloration phenomenon is a main concern in laser cleaning bronze [60]. Whether and to what extent the typical micromelting happened is decisive in evaluating the suitability of laser cleaning. Figure 11a and b were photographed using respectively magnification of 20 × and 10 × of the employed microscope device, while Fig. 12 was taken using magnification around 60x, which

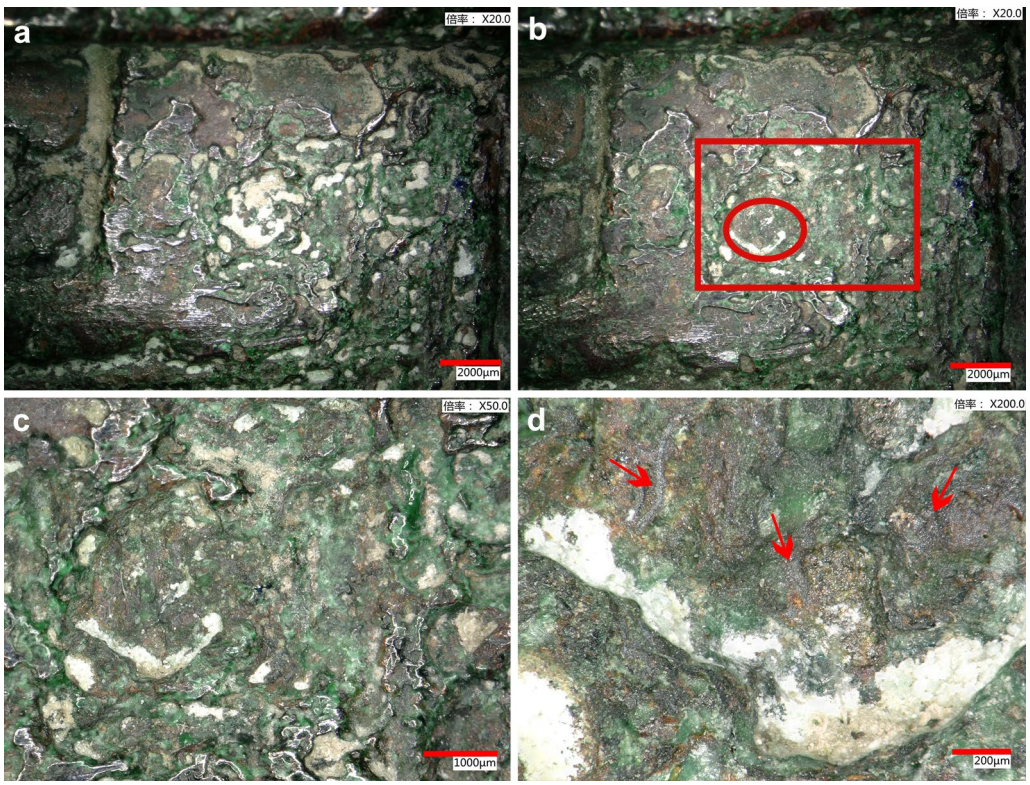

Fig. 13 Areas before (**a**) and after (**b**) cleaning under magnification of 20x. Scale bar: 2000 μm. The rectangular area corresponded with the view of (**c**) under magnification of 50x (scale bar: 1000 μm), the oval area corresponded with the view (**d**) under magnification of 200x (scale bar: 200 μm), with red arrows pointing at the suspected micromelting

were within the limit of perception of naked eye observation. The dimension of this object excluded the possibility of observation under SEM–EDS, further magnifications with video microscopes were used to observe the area after cleaning. As shown in Fig. 13, no alteration sign was observed under the magnification of 50x. Only under the magnification of 200x, suspected micromelting in localized micro areas was observed, whilst most of the patina remained unaltered. From a practical view, alteration in such a scale could actually be taken as negligible, considering that the physical and/or chemical alteration risk of this microscopic level could hardly be excluded from any kind of intervention.

Although successful cases using SFR are also reported [2, 11, 14], in the present case this regime required much higher fluence to remove the material and was much less efficient than the LQS mode, whilst leading to thermal effects even with wetting agent. Evident micromelting, discoloration, and partial removal of patina were observed (Fig. 14). It was therefore considered improper for this bronze. The thermal damage was probably due to the reduction of metal heating of this longer pulse, accompanied with increase of cleaning threshold and consequent risk of massive heating [2].

In parallel with the initial trial on the bronze, further study on the mechanism of laser-material interaction was conducted to explore eventual reference significance of this case. Corundum powders are reported to be insensitive and transparent for the 1064 nm wavelength of Nd:YAG laser [61, 62]. Laser beam was found to penetrate directly Elvax 40W and another poly (ethylene-*co*-acrylic acid) polymer samples during the experiment. The reason why laser irradiation worked on the mixture material on bronze, but not on the mock-up samples, might be various. The explosive evaporation of the wetting agent during the first one or two pulses could bring away part of superficial particles through transient forces [63]. During the following pulses when wetting agent already evaporated, spallation was very likely to happen, considering the ejection of flake-like debris during the cleaning of this bronze. Cuprite and malachite of the substrate, which were already formed before the application of these past interventions, absorbed the energy of penetrating laser, which led to the thermal expansion and further facilitated the detachment of the deposit materials [64]. What is more, the particles of corundum powder have been reported to act as lenses and create optical field enhancement effect [61], while the laser might still

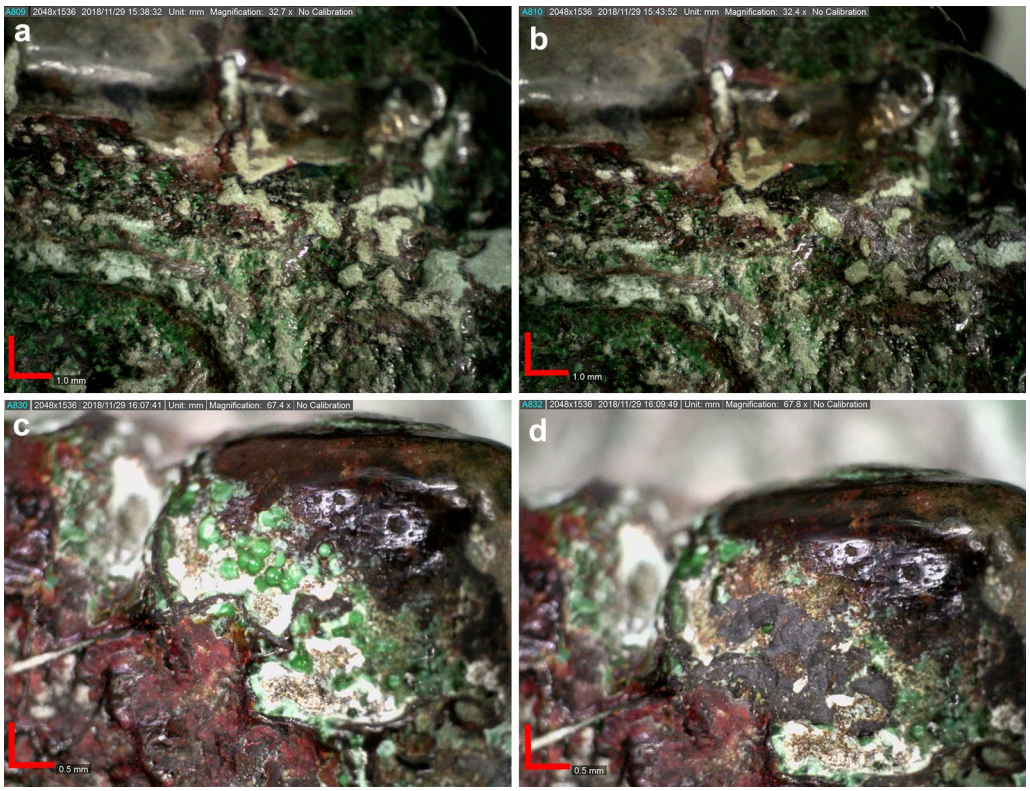

Fig. 14 Before (**a**, **c**) and after (**b**, **d**) laser cleaning of test areas with irradiation in SFR regime using the same spot size and frequency with LQS regime. **b** Inefficacy cleaning with localized discoloration using lower fluence (3.4 mJ/cm^2). **d** Removal of both unwanted material and patina with extensive discoloration using higher fluence (5.6 mJ/cm^2). Scale bar: 1.0 mm in (**a**) and (**b**), 5.0 mm in (**c**) and (**d**)

exercise thermal effect on the polymer of low-optical-absorbance [65].

Mock-up disk samples containing accessory components also revealed noteworthy phenomenon. Experimental irradiation on the mock-up samples showed that both cerussite and covellite are sensitive to laser. Covellite at a concentration of 1% (wt.) in corundum improved significantly the interaction between laser and material. Irradiation on the sample with 1% of cerussite in corundum caused only slight ablation traces which recovered almost immediately, but the cover slip put on the surface of the sample collected ejected materials during ablation, indicating that the laser-material interaction (Fig. 15) was significantly enhanced than on pure corundum. It was probable that, the ablation that happened to the reactive particles induced thermal load or mechanical wave, which in turn transferred to the surrounding particles.

Unlike the selective evaporation commonly observed in stone artifact cleaning, the spallation mechanism is not selective and less controllable [66]. The aforesaid lense effect and thermal load could also bring potential risk to the bronze substrate [64, 67]. However, the thickness of the deposit accumulation made this process less risky, while the wetting agent limited the thermal risk at least in the beginning of the ablation. To avoid eventual discoloration derived from excessive irradiation, it was chosen to limit strictly the pulse number as beforementioned. Despite the small part of deposit material sometimes left in the marginal area of the cavities, laser cleaning demonstrated evident advantages over the other methods for this case in efficacy, efficiency and safety.

Combined application of laser and chemical methods

In order to minimize the eventual micromelting, after using LQS regime with the above-mentioned parameters to remove the bulk of the multi-phase deposit, the irradiation was stopped and the cleaning was continued with the organic solvent to achieve further improvement in cleaning effect. The agent used was the mixture substituting tetrahydrofuran (43% isopropyl, 18% nonane and 39% methyl ethyl ketone), which worked slightly faster than the other one. It was delivered with wet compress for 15 min, followed by the brushing with medium stiff bristles. Residues thus brushed out of the cavities were taken away with cotton swab moistened with the same agent. This operation was repeated when necessary. When an adequate effect was obtained for the inside of cavities, the surrounding areas were also swabbed thoroughly with this mixture till no whitish aspect or sticky touch was perceived.

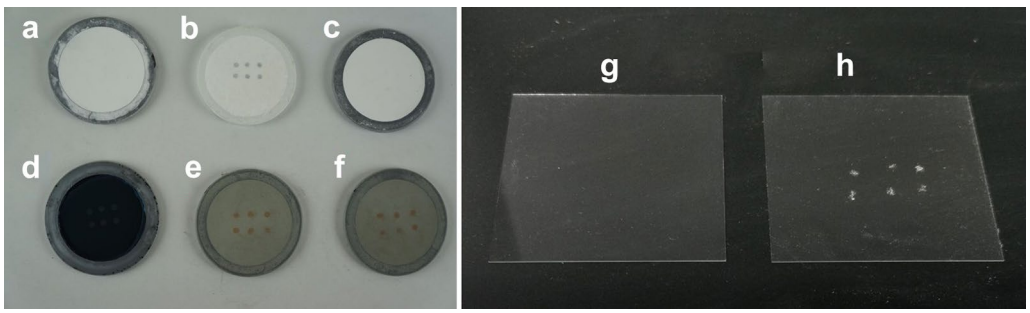

Fig. 15 Disk samples after laser ablation using the same spot and energy as on the bronze: **a** pure corundum, **b** pure cerussite. **c** 1% (wt.) cerussite in corundum, **d** pure covellite, **e** 1% (wt.) covellite in corundum and **f** 1% (wt.) covellite and 1% (wt.) cerussite in corundum. Cover slips put on the samples during laser ablation: **g** on the pure corundum pill and **h** for 1% (wt.) cerussite in corundum sample

Fig. 16 Area before (**a**) and after laser cleaning (**b**) and laser-chemical cleaning (**c**). Scale bar: 5.0 mm

Fig. 17 Different parts of the *Gu* vessel: before (**a**, **c**, **e**) and after cleaning with laser cleaning and residue removal with solvent mixture (**b**, **d**, **f**)

The combined application led to a cleaning result more thorough and homogeneous than laser used alone (Fig. 16). The bronze after cleaning had a homogeneous aspect and good legibility, with all the lustrous patina intact (Fig. 17).

Analysis for evaluating the cleaning effects

Besides direct observation, video microscope was the commonest instrument in cleaning result evaluation as seen in Figs. 11, 12, 13, 14 and 16, which supported the adoption of laser and laser-chemical methods.

Tentative analyses with Raman spectroscopy and hyperspectral imaging system were performed to introduce more objective dimensions in assessment. The Raman analysis was conducted on the areas analyzed in the preliminary diagnostic stage before cleaning. Given the impossibility of recording the spectra exactly from the same spot, more micro zones were analyzed to make up for this disadvantage in repeatability. Most of the spectra collected after cleaning were those of cuprite, malachite, azurite and sometimes cerussite, indicating that the pale green material has been removed from the bronze substrate. These results supported the efficacy of the cleaning. Although the preservation of the original substrate could be hardly verified in this way, the laser alteration product of bronze substrate, the tenorite (CuO) was not found in the test areas [2, 68]. Characteristic bands of aluminum oxide were found nowhere, while those of calcite and quartz were revealed in a few areas, indicating the residual earthy deposit. Only very few spectra still demonstrated the characteristic peak of the polymer in the range over 2700 cm^{-1} but quite deformed (Fig. 18). It could be confirmed in the qualitative dimension that the cleaning had successfully removed the unwanted materials while conserving the patina of original surface.

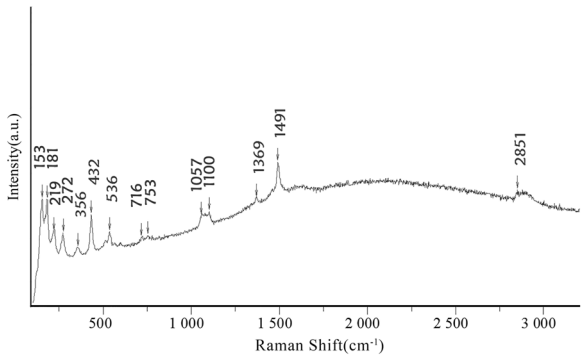

Fig. 18 Raman spectra obtained from one cleaned area revealed the malachite of the substrate and organic residue of deposit

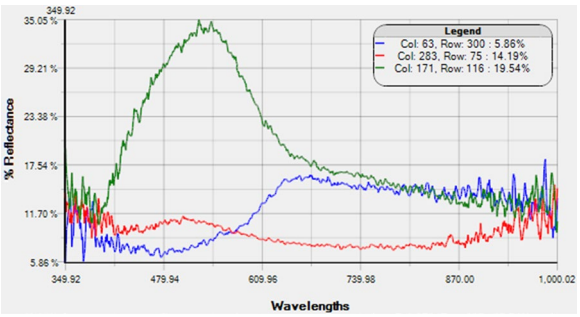

Fig. 20 Spectra acquired before cleaning. The green, blue and red colors on mapping images indicate unwanted materials, cuprite and malachite, respectively

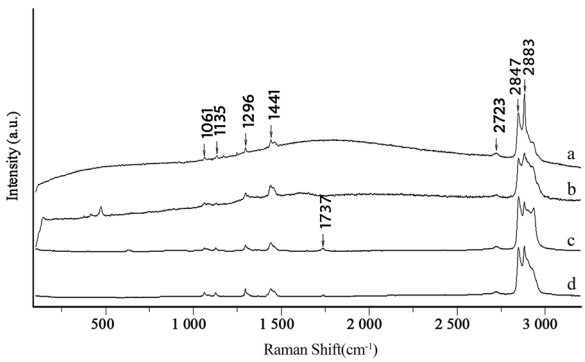

Fig. 19 Raman spectra of: **a** film-like debris collected during laser cleaning, **b** deposit on the *Gu* vessel, **c** Elvax 40W, **d** a poly (ethylene-*co*-acrylic acid) polymer

In addition, the Raman spectra of a larger flake of debris (about 1 mm^2) collected during the ablation confirmed the interpretation of the organic part in the preliminary investigation (Fig. 19). The spectrum of this film-like debris contained exactly the same bands with those over 1000 cm^{-1} in the spectra of the pale green material obtained before intervention, which indicated the absence of laser-induced decomposition or degradation generated and probably also limited thermal effect during the cleaning. The observed rupture and ejection of debris during laser cleaning was also reported in the literature on the removal of aged conservation material [10].

The hyperspectral imaging here was applied to the comparison between cleaning effects of laser-chemical and manual-chemical cleaning in a macroscopic level. The middle part of the *Gu*, which could be positioned parallel to the camera, was selected. The condition before intervention was documented through acquiring the spectral data of the unwanted materials, malachite and cuprite patina. Using these spectra as sampling references, distribution of these materials on the same areas was mapped after cleaning (Fig. 20). Although the slight deviation of image taking position introduced change of illumination and consequently some minor divergences present in the two mappings, the results were still illustrative: the green-colored area representing unwanted materials disappeared after cleaning with either of the methods, leaving the underlying malachite and cuprite visible. The analysis confirmed that with laser cleaning it is possible to achieve visual and qualitative effect comparable to manual cleaning on a macroscale, while saving three-fourths of the operation time (Fig. 21).

According to the encouraging results of all these analyses, it is possible to conclude that, although the laser-induced microscopic alteration could not be totally avoided, more effective cleaning in unit time could be achieved with laser than organic solvent and manual cleaning, while the respect towards original substrate is much better than ultrasonic ablator and chelants. With the assistance of organic solvent mixture as a post-treatment, the cleaning efficacy and visual effect after cleaning are further improved. The cleaning of the whole surface was then proceeded with the laser-chemical method.

Discussion

The adopted analytical itinerary proved to be adequate for the identification of the main compositions of the discussed unusual pale green material, which corresponded to different past interventions.

In specific, in-situ Raman spectroscopy analysis, through which fast and non-destructive examination of numerous areas of this *Gu* vessel was conducted, played a fundamental role in the revelation of the presence of both inorganic and organic compounds behind the "deceitful" aspect of the unusual material on surface and in the programming of subsequent investigation and intervention. In case the more conventional instrument for bronze degradation, XRD, were used at first, the presence of the

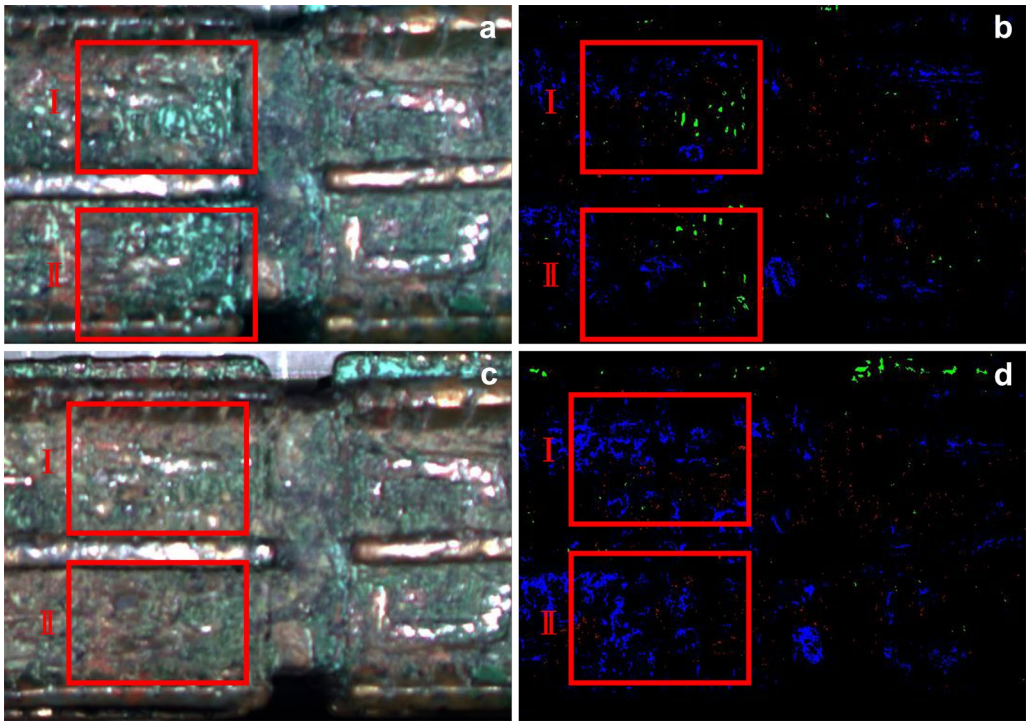

Fig. 21 Spectral Angle Mapper (SAM) classification was used. **a** and **c**: before cleaning; **b** and **d**: after cleaning. The rectangular I: area cleaned with laser-chemical method; the rectangular II: area cleaned with manual-chemical method. The colors indicate the same materials as in Fig. 20

organic part in the mixture is likely to be neglected, considering that XRD can hardly analyze the non-crystalline structure of many organic materials. The high sensitivity of Raman spectroscopy demonstrated advantage in revealing accessory components of low concentration, which XRD prone to miss out. Here the reasonable suggestion of the presence of covellite based on Raman results provided further guidance on mock-up samples preparation for studying the difference in Raman scatter yields among various compounds in mixture and the influence of accessory elements on laser-material interaction as well. Compared with other methods for the identification of organic materials, such as High Performance Liquid Chromatography-Mass Spectrometry, Raman analysis, with the features of being intuitive, rapid and sample-free, made the identification of the organic part in the mixture less laborious.

Guided by the results of preliminary analyses, the conservation strategy adopted here satisfied both the conservation need and visual integrity, and complied with the contemporary conservation trends for being residue-free and eco-friendly. The homogenous cleaning respecting the original patina of such a large surface demonstrated the practical utility of laser in removing the coating or material of external provenance from bronze, as reported in most of the successful cases [10–13], even when the main components of the unwanted material were not strong absorbers of the laser used. The successful application in this case might be attributable to multiple conditions: the significant difference in thermal conductivity between these materials and metal substrate, the clear boundary in the interface, the influence of laser-sensitive accessory components, and the absorbing underlying substrate, etc. The micromelting was observable only in microscopic level, as revealed in some other reported cases [58, 69], therefore was regarded as acceptable. It is also to note that recovery from this phenomenon over time is reported [70].

While Nd:YAG 1064 nm laser again proved its versatility in cleaning materials of various types, other operation parameters are significantly case-dependent [2, 3], considering the diversity in alloy composition and conservation condition among different bronzes, and the difference in pulse durations even belonging to the same regime among various apparatus. Although the pulse width of 100 ns used here has also been applied with success in some other cases with less thermal effect observed [9, 12], in other reports the longer pulses in SFR regime was found more suitable [3].

Even on the same object, as shown in this case, adjustment of parameters in spot size, fluence and pulse number was inevitable and actually necessary for adapting

to the complicated morphology of surface. Therefore, "manual skills" required in using conventional restoration manual utensils is also important for working with laser, for example, the operation with out-of-focus mode [58] which proved to be a safe operation mode especially when working with small spot is necessary. The timely cease of laser pulse is especially important for bronze, since the laser often works in a less selective mode on this kind of substrate [67]. As observed here, the initial exposure of the substrate should be taken as a sign for reducing pulse number or stopping irradiation, considering that another method could work well on the residue of unwanted material after the laser-induced rupture of its structure. Actually, the possibility of combining laser with other cleaning methods as one of the main optimization routes [12, 70] should be taken into account in the initial trial.

As for the cleaning effect evaluation, the Raman analysis also provided significant results in qualitative dimension, showing capability of revealing eventual residue of organic materials. Compared with portable XRF and portable FTIR already applied to the evaluation of laser and other cleaning intervention [11, 13, 71], the result of Raman spectroscopy is less representative for the micro dimension of its test area, but more precise for such a complicated and uneven surface of this *Gu* vessel. Examination of more areas could compensate the insufficiency in representativeness.

The hyperspectral imaging analysis conducted here documented in an intuitive and objective mode the entity of removed material and the condition of the substrate exposed after cleaning, giving indication on both the efficacy and safety of the intervention on macroscale. Elimination of the illumination deviation still demands more delicate strategy, such as using closed sample room and employing positioning.

Conclusions

The study provided reference for the optimization of investigation and conservation for the bronze artwork with similar situation, in which undocumented past interventions give rise to surface degradations much more complicated than usual corrosion products.

In-situ Raman analysis can give fast indications on the complexity in composition and help in optimizing the following diagnostic itinerary. The same instrument can also be a prospective method for qualitative assessment of cleaning effects on bronzes with complicated surface with unevenness.

The hyperspectral imaging analysis can actually investigate much larger area, therefore is a potential method for macroscale evaluation in both qualitative and visual dimensions.

The applicability of laser to the removal of materials of external provenance and the derived products in real bronze conservation task is a great advantage, since these materials are usually difficult to remove using conventional methods. The findings that various laser-material interactions different from the most familiar selective evaporation can happen on one hand indicates wider application prospects of laser, on the other calls for more attentive operation skills to limit the micromelting phenomenon. Combining laser and other methods demonstrated noteworthy practicability.

Considering that various degradation products and earthen contaminants are usually present in mixture on bronze surface, the simple but intuitive method of experimenting on mock-ups is significant for a better interpretation of complicated spectra, and exploration of the interaction between laser and mixed solid particles. The latter is still difficult to foreseen according to the existent studies on pigments [72], hence future mechanism study is needed.

Abbreviations

EDS	Energy dispersive spectroscopy
EDTA	Ethylene diamine tetraacetic acid
FTIR	Fourier transformed infrared
LQS	Long Q-switched
NIR	Near infrared
NUV	Near ultraviolet
SAM	Spectral angle mapper
SEM	Scanning electron microscopy
SFR	Short free running
XRD	X-ray diffraction
XRF	X-ray fluorescence
YAG	Yttrium aluminum garnet

Acknowledgements

The authors acknowledge the financial support from Shanghai Museum for the project "Research on the application of in-situ Raman spectroscopy analysis technique in the identification of corrosion products on bronze cultural relics". The authors express sincere gratitude to Prof. Ya Zhou and Prof. Jinhong Ma of the Bronze Study Department of Shanghai Museum for allowing us to work on this bronze *Gu* vessel of the museum's collection, to Prof. Hao Zhou, Prof. Zhongming Ding and Mr. Enyuan Wang of the Conservation Center of Shanghai Museum for providing manufacture technique background. Acknowledgements also go to Prof. Haifeng Yang of Shanghai Normal University for the precious help on the interpretation of Raman spectra.

Author contributions

YS: video microscope, Raman spectroscopy and SEM–EDS analyses. Chemical and laser cleaning. Mock-up sample preparation. Investigation and intervention management. Wrote the manuscript text. Prepared all figures except for Figs. 20 and 21. GZ: participation in cleaning comparative experiments design and cleaning extent checking. Mechanical cleaning. Revision of the text on mechanical cleaning. Provision of the information and reference on the traditional bronze intervention of polishing with agate spatula. XZ: hyperspectral imaging analysis. Prepared Figs. 20 and 21. Revision of the text on hyperspectral imaging. All authors read and approved the final manuscript.

Funding
This work was financially supported by Shanghai Museum research project "Research on the application of *in-situ* Raman spectroscopy analysis technique in the identification of corrosion products on bronze cultural relics".

Availability of data and materials
All data generated or analyzed during this study are included in the article.

Declarations

Ethics approval and consent to participate
Not applicable.

Consent for publication
Not applicable.

Competing interests
The authors declare that they have no competing interests.

Received: 30 December 2022 Accepted: 16 April 2023
Published online: 01 May 2023

References

1. Scott DA. Copper and bronze in art. Corrosion, colorants, conservation. Los Angeles: Getty Publications; 2002: p.322-6,359-60, 362-4.
2. Siano S, Agresti J, Cacciari I, Ciofini D, Mascalchi M, Osticioli I, Mencaglia AA. Laser cleaning in conservation of stone, metal, and painted artifacts: state of the art and new insights on the use of the Nd: YAG lasers. Appl Phys A. 2012;106(2):419–46.
3. Bertasa M, Korenberg C. Successes and challenges in laser cleaning metal artefacts: a review. J Cult Herit. 2022;53:100–17.
4. Korenberg C, Baldwin A. Laser cleaning tests on archaeological copper alloys using an ND: YAG Laser. Laser Chem. 2006. https://doi.org/10.1155/2006/75831.
5. De Giorgi M, D'Anna E, Della Patria A, De Rosa H, Lorusso A, Orfanou P, Perrone A. Laser cleaning of copper-based coins. In: Saunders D, Strlic M, Korenberg C, Luxford N, Birkholzer K, editors. Lasers in the Conservation of artworks—LACONA IX proceedings. London: Archetype; 2013. p. 192–3.
6. Buccolieri G, Nassisi V, Torrisi L, Buccolieri A, Castellano A, Di Giulio M, Giuffreda E, Delle Side D, Velardi L. Analysis of selective laser cleaning of patina on bronze coins. J Phys Conf Ser. 2014;508(1):012032.
7. Di Francia E, Lahoz R, Neff D, De Caro T, Angelini E, Grassini S. Laser-cleaning effects induced on different types of bronze archaeological corrosion products: chemical-physical surface characterization. Appl Surf Sci. 2022;573:150884.
8. Siatou A, Charalambous D, Argyropoulos V, Paraskevi P. A comprehensive study for the laser cleaning of corrosion layers due to environmental pollution for metal objects of cultural value: preliminary studies on artificially corroded coupons. Laser Chem. 2006. https://doi.org/10.1155/2006/85324.
9. Drakaki E, Klingenberg B, Serafetinides AA, Kontou E, Katsikosta N, Tselekas P, Evgenidou D, Boukos N, Zanini A. Evaluation of laser cleaning of ancient Greek, Roman and Byzantine coins. Surf Interface Anal. 2010;42(6–7):671–4.
10. Dajnowski A, Lins A. The practical use of lasers in removing deteriorated Incralac coatings from large bronze monuments. In: Radvan R, Asmus JF, Castillejo M, Pouli P, Nevin A, editors. Lasers in the conservation of artworks VIII. London: CRC; 2011. p. 47–52.
11. Sansonetti A, Colella M, Letardi P, Salvadori B, Striova J. Valutazione analitica degli effetti di una pulitura laser: la statua in bronzo di Napoleone come Marte Pacificatore di Antonio Canova (Analytical evaluation of the effects of laser cleaning: the bronze statue of Napoleon as Mars the Peacemaker by Antonio Canova). In: Brunetto A, editor. Aplar 5 Applicazioni laser nel restauro (Aplar 5 Laser applications in restoration). Atti del Convegno (Conference proceedings). Firenze: Nardini; 2017. p. 297–307 (in Italian).
12. Shen Y, Bassilisi V, Paderni L. Laser cleaning of Japanese bronze mirrors from the Luigi Pigorini National Museum of Prehistory and Ethnography. In: Brunetto A, Lanterna G, Mazzei B, editors. Aplar 6 Applicazioni laser nel restauro (Aplar 6 Laser applications in restoration). Atti del Convegno (Conference proceedings). Firenze: Nardini; 2019. p.339–53.
13. Basso E, Pozzi F, Reiley MC. The Samuel F. B. Morse statue in Central Park: scientific study and laser cleaning of a 19th-century American outdoor bronze monument. Herit Sci. 2020;8:81.
14. Pini R, Siano S, Salimbeni R, Pasquinucci M, Miccio M. Tests of laser cleaning on archeological metal artefacts. J Cult Herit. 2000;1:S129–37.
15. Hou M, Pan N, Ma Q, He H, Lü S, Hu Y. Review of hyperspectral imaging technology in analyzing pained artifacts. Spectrosc Spect Anal. 2017;37(6):1852–60.
16. Picollo M, Cucci C, Casini A, Stefani L. Hyper-spectral imaging technique in the cultural heritage field: New possible scenarios. Sensors. 2020;20(10):2843.
17. Kubik M. Hyperspectral imaging: a new technique for the non-invasive study of artworks. In: Creagh D, Bradley D, editors. Physical techniques in the study of art, archaeology and cultural heritage, vol. 2. Amsterdam: Elsevier; 2007. p. 199–259.
18. Di B, Messinger DW, Howell D. Hyperspectral analysis of cultural heritage artifacts: pigment material diversity in the Gough map of Britain. Opti Eng. 2017;56(8):081805.
19. Liu X, Chen M, Liu Y. Application of hyperspectral imaging technique in identification of polymer-impregnated gemstone: taking jadeite and turquoise as example. J Gems Gemmol. 2019;21(1):1–11 (in Chinese).
20. He T. History of engineering and technology of metallurgy and metalworking in ancient China. Taiyuan: Shanxi Jiaoyu; 2009. p. 113–24 (in Chinese).
21. Mei J, Chen K, Cao W. Scientific examination of Shang-dynasty bronzes from Hanzhong, Shaanxi Province. China J Archaeol Sci. 2009;36(9):1881–91.
22. Scott DA. A review of copper chlorides and related salts in bronze corrosion and as painting pigments. Stud Conserv. 2000;45(1):39–53.
23. Coladonato M, Scarpitti P. Note sul triangolo interattivo dei solventi e delle solubilità© (Notes on the interactive triangle of solvents and solubilities). (Istituto Centrale per il Restauro), http://www.icr.beniculturali.it/flash/progetti/TriSolv/dati/IT/TriSolv_IT.pdf. Accessed 1 Dec 2022 (in Italian).
24. He L, Zhao Q, Gao M. Characterization of corroded bronze Ding from the Yin Ruins of China. Corros Sci. 2007;49(6):2534–46.
25. Cao C. Study on the descendants group of ancient bronze Zhang faction in Shanghai in the bronze restoration and imitation field. Master's thesis. Nanjing University of Information Science and Technology. 2018; p. 24 (in Chinese).
26. Strobl RG, Hagedorn W. Raman spectroscopic method for determining the crystallinity of polyethylene. J Polym Sci Poly Phys Ed. 1978;16(7):1181–93.
27. Shimoyama M, Maeda H, Matsukawa K, Inoue H, Ninomiya T, Ozaki Y. Discrimination of ethylene/vinyl acetate copolymers with different composition and prediction of the vinyl acetate content in the copolymers using Fourier-tansform Raman spectroscopy and multivariate data analysis. Vib Spectrosc. 1997;14:253–9.
28. Miranda AM, Castillo-Almeida EW, Martins Ferreira EH, Moreira GF, Achete CA, Armond RASZ, Dos Santos HF, Jorio A. Line shape analysis of the Raman spectra from pure and mixed biofuels esters compounds. Fuel. 2014;115:118–25.
29. Guo J, Guo L, Chen W. Raman spectra of minerals. Beijing: Geology Press; 2016. p. 32–5 (in Chinese).
30. Gallas MR, Chu YC, Piermarini GJ. Calibration of the Raman effect in α-Al_2O_3 ceramic for residual stress measurements. J Mater Res. 1995;10(11):2817–22.
31. Porto SP, Krishnan RS. Raman effect of corundum. J Chem Phys. 1967;47(3):1009–12.
32. Li PG, Lei M, Tang WH. Raman and photoluminescence properties of α-Al_2O_3 microcones with hierarchical and repetitive superstructure. Mater Lett. 2010;64(2):161–3.
33. Guo J, Guo L, Chen W. Raman spectra of minerals. Beijing: Geology Press; 2016. p. 23 (in Chinese).
34. Sander T, Reindl CT, Klar PJ. Breaking of Raman selection rules in Cu_2O by intrinsic point defects. MRS Online Proc Libr. 2014;1633:81–6.

35. Guo J, Guo L, Chen W. Raman spectra of minerals. Beijing: Geology Press; 2016. p. 59 (in Chinese).
36. Martens WN, Rintoul L, Kloprogge JT, Frost RL. Single crystal raman spectroscopy of cerussite. Am Miner. 2004;89(2–3):352–8.
37. Parker G, Hope GA, Woods R. Raman spectroscopic identification of surface species in the leaching of chalcopyrite. Colloid Surf A. 2008;318:160.
38. Milekhin AG, Yeryukov NA, Sveshnikov LL, Duda TA, Rodyakina EE, Gridchin VA, Sheremet ES, Zahn DRT. Combination of surface-and interference-enhanced Raman scattering by CuS nanocrystals on nanopatterned Au structures. Beilstein J Nanotech. 2015;6(1):749–54.
39. Jia Y, Sciutto G, Prati S, Catelli E, Galeotti M, Porcinai S, Mazzocchetti L, Samorì C, Galletti P, Giorgini L, Tagliavini E, Mazzeo R. A new bio-based organogel for the removal of wax coating from indoor bronze surfaces. Herit Sci. 2019;7:34.
40. Viljus A, Viljus M. The conservation of Early Post-medieval Period coins found in Estonia. J Conserv Mus Stud. 2012;10:30–44.
41. Baij L, Hermans J, Ormsby B, Noble P, Iedema P, Keune K. A review of solvent action on oil paint. Herit Sci. 2020;8:43.
42. Casoli A, Di Diego Z, Isca C. Cleaning painted surfaces: evaluation of leaching phenomenon induced by solvents applied for the removal of gel residues. Environ Sci Pollut Res. 2014;21:13252–63.
43. Moretti P, Cartechini L, Miliani C. Single-sided NMR: a non-invasive diagnostic tool for monitoring swelling effects in paint films subjected to solvent cleaning. Anal Bioanal Chem. 2020;412:1063–75.
44. Burtch NC, Jasuja H, Walton KS. Water stability and adsorption in metal-organic frameworks. Chem Rev. 2014;114:10575–612.
45. Feng PL, Perry JJ IV, Nikodemski S, Jacobs BW, Meek ST, Allendorf MD. Assessing the purity of metal-organic frameworks using photoluminescence: MOF-5, ZnO quantum dots, and framework decomposition. J Am Chem Soc. 2010;132:15487–9.
46. Safy MEA, Amin M, Haikal RR, Elshazly B, Wang J, Wang Y, Wöll C, Alkordi MH. Probing the water stability limits and degradation pathways of metal-organic frameworks (MOFs). Chem Eur J. 2020;26:7109–17.
47. Shao L, et al. Analytical chemistry. Beijing: Higher Education Press; 1995. p. 135–50 (in Chinese).
48. Campanella L, Cardellicchio F, Dell'Aglio E, Reale R, Maria SA. A green approach to clean iron stains from marble surfaces. Herit Sci. 2022;10:79.
49. Degrigny C. Use of electrochemical techniques for the conservation of metal artefacts: a review. J Solid State Electrochem. 2010;14:353–61.
50. Macchia A, Sammartino MP, Tabasso L. A new method to remove copper corrosion stains from stone surfaces. J Archaeol Sci. 2011;38(6):1300–7.
51. Spile S, Suzuki T, Bendix J, Simonsen KP. Effective cleaning of rust stained marble. Herit Sci. 2016;4:12.
52. Spile S, Suzuki T, Bendix J, Simonsen KP. Effective cleaning of copper stained calcareous stone. Herit Sci. 2016;4:29.
53. Ryczkowski J. EDTA interaction with γ-alumina. React Kinet Catal L. 1993;51(2):501–6.
54. Coskuner O, Jarvis EAA. Coordination studies of Al-EDTA in aqueous solution. J Phys Chem A. 2008;112(12):2628–33.
55. Turner-Walker G. A practical guide to the care and conservation of metals. Taipei: Xi Wang Art and Design Agency; 2008. p. 65, 69-70.
56. Turner-Walker G. The nature of cleaning: physical and chemical aspects of removing dirt, stains and corrosion. In: proceedings of the international symposium on cultural heritage conservation. Tainan: 6th-8th November. 2012. https://www.researchgate.net/publication/235788601_The_nature_of_cleaning_physical_and_chemical_aspects_of_removing_dirt_stains_and_corrosion. Accessed 1 Dec 2022.
57. Scholten JH, Teule JM, Zafiropulos V, Heeren RMA. Controlled laser cleaning of painted artworks using accurate beam manipulation and on-line LIBS-detection. J Cult Herit. 2000;1:S215–20.
58. Croveri P, Demmelbauer M, Poli T, Cavaleri T, Giovagnoli A, Chiantore O. La pulitura laser di leghe metalliche di interesse artistico: modificazioni morfologiche e chimiche di superfici patinate e non (Laser cleaning of metal alloys of artistic interest: morphological and chemical modifications of patinated and non-patinated surfaces). In: Brunetto A, editor. Aplar 4 Applicazioni laser nel restauro (Aplar 4 Laser applications in restoration). Atti del Convegno (Conference proceedings). Padua: Il prato; 2013. p. 295–306. (in Italian)
59. Theodorakopoulos C. The excimer laser ablation of picture varnishes: an evaluation with reference to light-induced deterioration. PhD dissertation. Royal College of Art, 2005.
60. Siano S, Salimbeni R. Advances in laser cleaning of artwork and objects of historical interest: the optimized pulse duration approach. Accounts Chem Res. 2010;43(6):739–50.
61. Mosbacher M, Münzer HJ, Zimmermann J, Solis J, Boneberg J, Leiderer P. Optical field enhancement effects in laser-assisted particle removal. Appl Phys A. 2001;1:41–4.
62. Chappé M, Hildenhagen J, Dickmann K, Bredol M. Laser irradiation of medieval pigments at IR, VIS and UV wavelengths. J Cult Herit. 2003;4:264–70.
63. Tam AC, Leung WP, Zapka W, Ziemlich W. Laser-cleaning techniques for removal of surface particulates. J Appl Phys. 1992;71(7):3515–23.
64. Madden O, Abraham M, Scheerer S, Werden L. The effects of laser radiation on adhesives, consolidants, and varnishes. In: Dickmann K, Fotakis C, Asmus JF, editors. LACONA V proceedings. Berlin: Springer; 2005. p. 247–54.
65. Ravi-Kumar S, Lies B, Zhang X, Lyu H, Qin H. Laser ablation of polymers: a review. Polym Int. 2019;68(8):1391–401.
66. Pouli P. Laser cleaning studies on stonework and polychromed surfaces. Dissertation. Loughborough University; 2000. p. 7–8,25–6.
67. Garbacz H, Fortuna-Zaleśna E, Marczak J, Strzelec M, Koss A, Zatorska A. Evaluation of laser cleaning of old copper roofing and gilding using tunable length laser pulse. In: Saunders D, Strlic M, Korenberg C, Luxford N, Birkholzer K, editors. Lasers in the Conservation of Artworks—LACONA IX proceedings. London: Archetype; 2013. p. 204–6.
68. Andriani SE, Iacobellis VN, Boraccesi G, La Notte G, Vona F, Daurelio G, Sibillano T, Schiavulli L, Catalano IM. L'intervento laser di pulitura e saldatura di una croce astile del Museo Diocesano di Bisceglie (The laser intervention of cleaning and welding of a processional cross of the Diocesan Museum of Bisceglie). Brunetto A, editor. Aplar 4 Applicazioni laser nel restauro (Aplar 4 Laser applications in restoration). Atti del Convegno (Conference proceedings). Padua: Il prato; 2013. p.307–26. (in Italian)
69. Jiang D, Luo Y, Gao M. Study on the removal of corrosion products on bronze relics using pulsed laser. J Northwest Univ. 1986;16(4):19–23 (in Chinese).
70. Froidevaux M, Platt P, Cooper M, Watkins K. Laser interactions with copper, copper alloys and their corrosion products used in outdoor sculpture in the United Kingdom. In: Castillejo M, Moreno P, Oujja M, Radvan R, Ruiz J, editors. Lasers in the conservation of artworks, LACONA VII proceedings. London: CRC Press; 2008. p. 277–84.
71. Buccolieri G, Nassisi V, Buccolieri A, Vona F, Castellano A. Laser cleaning of a bronze bell. Appl Surf Sci. 2013;272:55–8.
72. Bordalo R, Morais PJ, Young CRT, Santos LF, Almeida RM. Characterisation of laser-induced physical alterations of pigmented oil layers. e Preserv Sci. 2012;9:47–59.

Publisher's Note